Volume 27
Number 25
December 14, 1988

Inorganic Chemistry

Communications

Characterization of Nickel(II)–Nickel(IV) Linear-Chain Compounds by Nickel and Chlorine K-Edge EXAFS

Sir:

Mixed-valence linear-chain materials are currently an area of intensive study, with considerable technological interest due to their anisotropic optical and electrical conduction properties. Characterization of many of these materials has been difficult due to difficulties in obtaining single crystals and also crystallographic disorder. We report the use of metal and halogen absorption edge extended X-ray absorption fine structure (EXAFS) to exemplify the applicability of this technique to these problems and also to establish structural parameters for Ni(II)–Ni(IV) mixed-valence compounds.

Examples of platinum(II)–platinum(IV) compounds of this type have been known for many years, e.g. Wolffram's red salt $[Pt(H_2EtN)_4Cl_2][Pt(H_2EtN)_4]Cl_4{\cdot}4H_2O$, first prepared in 1900,[1] and more recently palladium(II)–palladium(IV),[2] palladium–platinum,[2a] and nickel–platinum[3] analogues have been characterized. The nickel(II)–nickel(IV) diamine complexes of this type were prepared in 1965,[4] although their true nature as mixed-valence class II materials was not recognized until 1981.[5] The nickel-based systems are potentially very important since they use a cheaper metal and appear to have higher electrical conductivities.[5] Studies of the nickel systems are considerably harder than for the Pt/Pd analogues for three reasons. First, in addition to mixed-valence Ni(II)–Ni(IV) materials, discrete Ni(III) complexes can be prepared; for example, ethylenediamine (en) produces both $[Ni^{III}(en)_2Cl_2]Cl$ (**1**) and $[Ni^{II}(en)_2][Ni^{IV}(en)_2Cl_2]Cl_4$ (**2**), while some other diamines have so far afforded only one type—$[Ni^{III}\{H_2N(CH_2)_3NH_2\}_2Cl_2]Cl$ (**3**) or $[Ni^{II}\{H_2NCH(Me)CH_2NH_2\}_2][Ni^{IV}\{H_2NCH(Me)CH_2NH_2\}_2Cl_2]Cl_4$ (**4**).[5,6] How changes in the diamine geometry and the reaction conditions control the nature of the products is imperfectly understood at present. Second, unlike the Pd or Pt systems, discrete Ni(IV) diamine complexes have not been obtained,[6,7] which limits the synthetic routes and the spectroscopic data available for comparison purposes. Finally, once formed, the mixed-valence nickel complexes are insoluble in, or decomposed by, common solvents, and attempts to obtain single crystals from in situ syntheses for an X-ray study have so far failed. Structural data can be derived in the absence of single crystals by EXAFS features of the metal or, perhaps, the halogen X-ray absorption edges. Here we report nickel and chlorine K-edge EXAFS studies of some of these nickel materials.

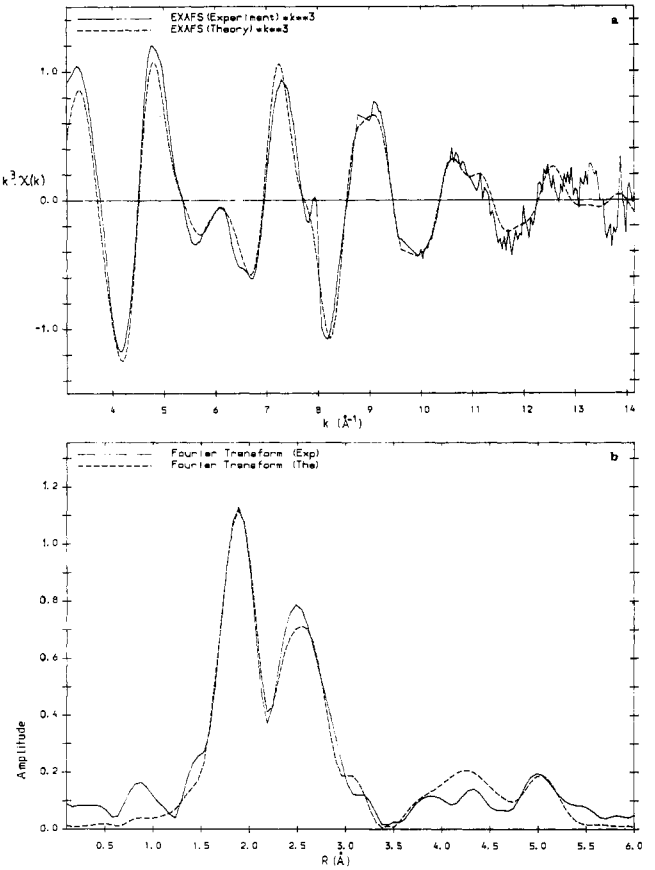

Figure 1. Experimental (—) and theoretical (- - -) nickel K-edge EXAFS data for $[Ni^{IV}(en)_2Cl_2Ni^{II}(en)_2]Cl_4$ (**2**): (a) k^3-weighted EXAFS; (b) Fourier transform of the data phase-shift-corrected for nitrogen. The theoretical fit was determined on Fourier-filtered data.

X-ray absorption spectra of compounds **1**, **2**, and **4** were recorded at ambient temperature on the Synchrotron Radiation Source at the SERC Daresbury Laboratory. Nickel K-edge spectra were recorded in transmission mode on beam line 7 with use of an order-sorting Si(111) monochromator;[8] the chlorine K-edge spectrum of **2** was recorded in vacuo on beam line 3 by means of a Ge(111) order-sorting monochromator using

(1) Millar, J. S. Ed. *Extended Linear Chain Compounds*; Plenum Press: New York, 1982; Vol. 1–3.
(2) (a) Matsumoto, N.; Yamashita, M.; Kida, S. *Bull Chem. Soc. Jpn.* **1978**, *51*, 2334. (b) Clark, R. J. H.; Croud, V. B.; Kurmoo, M. *Inorg. Chem.* **1984**, *23*, 2499.
(3) Clark, R. J. H.; Croud, V. B. *Inorg. Chem.* **1986**, *25*, 1751.
(4) Barbaeva, A. V.; Baranovskii, I. B.; Afanaseva, G. G. *Russ. J. Inorg. Chem.* (*Engl. Transl.*) **1965**, *10*, 1268.
(5) Yamashita, M.; Nonaka, Y.; Kida, N. S.; Hamaue, Y.; Aoki, R. *Inorg. Chim. Acta* **1981**, *52*, 43.
(6) Cooper, D. A.; Higgins, S. J.; Levason, W. *J. Chem. Soc., Dalton Trans.* **1983**, 2131.
(7) The *only* Ni(IV) complexes with neutral ligands currently isolated are with a restricted range of diphosphine and diarsine ligands: Higgins, S. J.; Levason, W.; Feiters, M. C.; Steel, A. T. *J. Chem. Soc., Dalton Trans.* **1986**, 317 and references therein.
(8) Greaves, G. N.; Diakun, G. P.; Quinn, P. D.; Hart, M.; Siddons, D. P. *Nuclear Instrum. Methods Phys. Res.* **1983**, *208*, 335.

0020-1669/88/1327-4521$01.50/0

Table I. EXAFS-Derived Parameters for Nickel Diamine Complexes: Internuclear Distance r (Å) and Debye–Waller Factor α (Å^2)[a]

	1		2		4	
shell	r	α	r	α	r	α
Ni–N	1.93 (1)	0.0067 (3)	1.91 (1)	0.011 (1)	1.91 (1)	0.0099 (3)
Ni–Cl	2.37 (1)	0.0129 (5)	2.37 (1)	0.007 (1)	2.37 (1)	0.0060 (5)
Cl–Ni^{IV}			2.37 (1)	0.0096 (3)		
Ni···C$_{ring}$	2.77 (1)	0.012 (1)	2.71 (1)	0.007 (1)	2.70 (1)	0.010 (1)
Ni^{II}···Cl			2.97 (1)	0.016 (1)	2.93 (1)	0.013 (2)
Cl···Ni^{II}			2.90 (1)	0.022 (3)		
Cl···N			3.10 (1)	0.0061 (6)		
Ni···Cl			3.88 (1)	0.009 (1)		
Ni···Cl			4.18 (1)	0.015 (1)		
Ni···Cl			4.36 (1)	0.018 (1)		
Ni···Ni			4.94 (1)	0.016 (1)	4.93 (1)	0.013 (2)

[a] $\alpha = 2\sigma^2$, where σ = mean square deviation in internuclear distance. R factors (calculated as in ref 11) for the Ni spectra were 15, 11, and 14% for **1**, **2**, and **4**. The absorbing atom is listed first. Standard deviations are in parentheses. The calculated standard deviations, which assume no parameter correlation, were checked for correlation effects by using the method in ref 12 and found to be within the bounds given.

fluorescence detection.[9] Analysis of the data was performed using spherical wave methods employing ab initio phase shifts and backscattering factors with the facility for the inclusion of multiple scattering effects.[10] The results are presented in Table I.

The EXAFS associated with the Ni K-edge provided evidence for the chelate ring in both the ethylenediamine complexes **1** and **2**, with the back-scattering from the carbon backbone evident, in addition to the expected Ni–N shell. The best means of differentiating the Ni(III) and Ni(II)–Ni(IV) isomers is to consider the Ni–Cl distances and any more distant shells. For the mixed-valence isomer **2**, both the Ni^{IV}–Cl and Ni^{II}···Cl distances were apparent, and their distances were refined to values of 2.37 and 2.97 Å, respectively. The experimental and modeled EXAFS spectra and their Fourier transforms are presented in Figure 1. The observation of the longer of these two shells is crucial to the characterization of this as a class II mixed-valence material. Application of the statistical criteria for the significance of a putative shell[11,12] and attempted fits of alternative models on two independent data sets both confirmed its validity. Further confirmation of this was provided by the chlorine K-edge EXAFS (−115 °C). For that absorbing element, only one-third of the sites are part of the –Ni–Cl···Ni··· chain, but the distances to nickel will be the shortest ones in the structure, and these were clearly apparent in the Fourier transform of the Cl K-edge EXAFS spectrum (Figure 2). The Ni^{IV}–Cl distances derived from the two edges were identical within experimental error. A discrepancy of 0.07 Å was derived for the Ni^{II}···Cl distance. However, at both edges another shell from a light element interferes with the analysis, resulting in a higher uncertainty, but without being so severe as to cast serious doubt about the existence of this shell. Very similar results were derived for the second mixed-valence material studied, compound **4**, at the nickel K-edge. Again there was strong evidence for the presence of the alternating nickel–chlorine internuclear distances along the linear chain.

These bond lengths may be compared to those of the Ni(II) analogue $[(\mu\text{-Cl})_2\{\text{Ni(en)}_2\}_2]\text{Cl}_2$.[13] In that structure, the mean Ni–N bond length is 2.10 Å, substantially longer than the values in these oxidized complexes. The Ni^{II}–μ-Cl distances (2.471 and 2.561 Å) are straddled by the shorter Ni^{IV}–Cl and Ni^{II}···Cl distances in the mixed-valence system **2**. Established Ni(III) and Ni(IV) sites have been characterized with heavier group 15 donor ligands, and these show Ni^{III}–Cl and Ni^{IV}–Cl distances of 2.4 and 2.28 Å, respectively.[7] The EXAFS-derived Ni^{III}–Cl bond length for **1** agrees closely with this, although the remaining ligands differ; it appears then that the Ni^{IV}–Cl separation in the two mixed-valence materials is lengthened by ca. 0.1 Å in the unsymmetrical linear bridge.

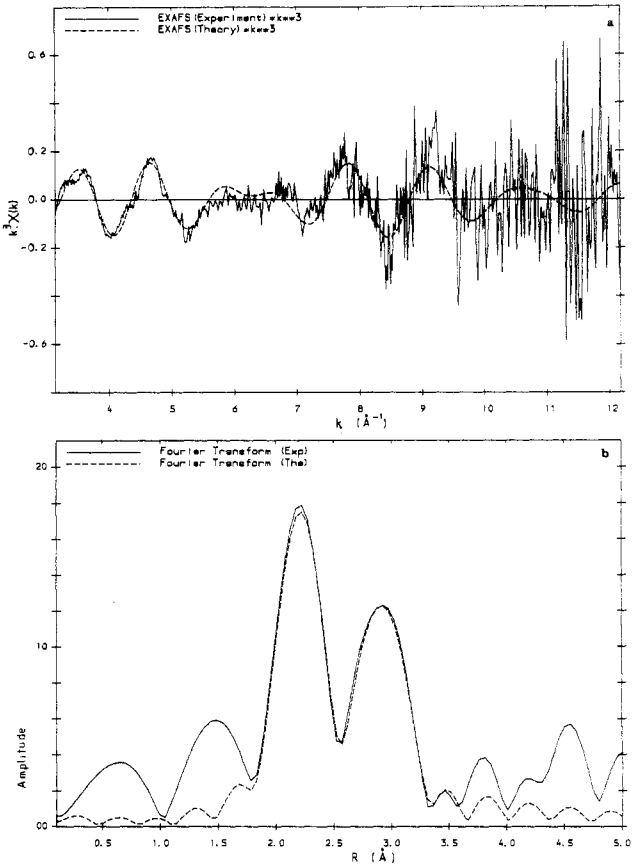

Figure 2. Chlorine K-edge EXAFS data for complex **2**. The presentation is as for Figure 1, except that there is k^2 weighting of the EXAFS data and the Fourier transform is phase-shift-corrected for nickel.

In principle, longer range distances could provide information about the lattice structure of these mixed-valence materials. The third shell evident in chlorine EXAFS of complex **2** can be attributed to a first-row element; it seems probable that this emanates from the coordinated nitrogens. The refined internuclear distance of 3.10 Å is appropriate for the separation within the Ni(IV) coordination center. Hydrogen bonding between the amine protons and the chloride counterions can also afford relatively short Cl···N separations in the region of 3.2 Å,[14] and these may also contribute to this shell. On a site population basis this will outweigh Cl···N backscattering from the intrachain halide center. The nickel edge data for both mixed-valence complexes displayed peaks in the Fourier transform near 5 Å. This is close to the sum

(9) MacDowell, A. A.; West, J. B.; Greaves, G. N. *Daresbury Laboratory Preprint*, DL/SCI/P557E; *Rev. Sci. Instrum.*, submitted for publication.
(10) Gurman, S. J.; Binsted, N.; Ross, I. *J. Phys. C* **1984**, *17*, 143; **1986**, *19*, 1845.
(11) Binsted, N.; Cook, S. L.; Evans, J.; Greaves, G. N.; Price, R. J. *J. Am. Chem. Soc.* **1987**, *109*, 3669.
(12) Joyner, R. W.; Martin, K. J.; Meehan, P. *J. Phys. C* **1987**, *20*, 4005.
(13) Joung, K. O.; O'Connor, C. J.; Sinn, E.; Carlin, R. L. *Inorg. Chem.* **1979**, *18*, 804.
(14) Craven, M. D.; Hall, D. *Acta Crystallogr.* **1961**, *14*, 475. Larsen, K. D.; Toftlund, H. *Acta Chem. Scand.* **1977**, *31A*, 182.

of the two nickel–chlorine distances and so may be attributable to the adjacent nickel in the linear chain, again according to fit index ratio,[12] integrated area,[11] and correlation[11] tests. Multiple scattering effects were found to have little effect on the analysis of this minor shell. At the present stage of analysis the angle at chlorine has been refined to ca. 140°, but this is a small component of the total EXAFS and this value is open to some doubt. Other small shells were reproducibly apparent in the Fourier transform of the nickel edge EXAFS of **2**; these seem likely to be due to the chloride counterions between the nickel–chlorine chains.

These results confirm complexes **2** and **4** as mixed-valence materials and offer the first structural details about them. They also demonstrate that EXAFS may be valuably applied to the study of such materials; the results of the experimentally more difficult chlorine SOXAFS (soft X-ray absorption fine structure) data are particularly encouraging. The observation of backscattering atoms out to ca. 5 Å from the absorbing metal center suggests that EXAFS may be used constructively in conjunction with X-ray powder diffraction to derive considerable detail about the lattice structures of these linear-chain compounds.

Acknowledgment. We wish to thank the SERC for access to the facilities of their Daresbury Laboratory and for support for J.T.G. and Richard Perry for some of the samples.

Supplementary Material Available: X-ray absorption spectra of $[Ni(en)_2Cl_2]Cl$ (Ni K-edge), $[Ni(en)_2Cl_2][Ni(en)_2]Cl_4$ (Ni K-edge), $[Ni\{H_2NCH(Me)CH_2NH_2\}_2Cl_2][Ni\{H_2NCH(Me)CH_2NH_2\}_2]Cl_4$ (Ni K-edge), and $[Ni(en)_2Cl_2][Ni(en)_2]Cl_4$ (Cl K-edge) in graphical and listing forms (36 pages). Ordering information is given on any current masthead page.

Department of Chemistry
The University
Southampton SO9 5NH, U.K.

John Evans*
J. Trevor Gauntlett
William Levason

Received July 8, 1988

Synthesis of High-Surface-Area α-$LiAlO_2$

Sir:

We have previously reported the room-temperature synthesis of lithium dialuminate, $[LiAl_2(OH)_6]^+(OH)^-\cdot 2H_2O$, by the imbibition of LiOH into bayerite, $Al(OH)_3$, in the molar ratio of 1:2.[1] Because $[LiAl_2(OH)_6]^+(OH)^-\cdot 2H_2O$ retains the layered structure of bayerite, it can react further with soluble salts in a second salt imbibition step. A material prepared with a Li:Al ratio of 1:1 would be a potential precursor for $LiAlO_2$.

$LiAlO_2$ adopts three different structures, the hexagonal α phase, the orthorhombic β phase, and a tetragonal γ phase. These three polymorphs form under similar reaction conditions, and mixtures of these polymorphs are commonly encountered in syntheses performed below 700 °C.[2] Above this temperature, the α- and β-polymorphs begin to convert to the γ-polymorph. The slow kinetics of this conversion make it difficult to identify the transition temperature, but by 900 °C the transformation is generally complete.

The thermal history of polycrystalline oxide materials plays a significant factor in determining their surface area. Conventional solid-state synthetic methods, which require higher temperature to reach complete reaction, yield products that have been desurfaced through sintering. For example, α-$LiAlO_2$ produced by the reaction of Li_2CO_3 with boehmite (AlO(OH)) at 600 °C for 30 h has a platelike morphology with particle size in the range of 1–25 μm and a surface area of less than 5 m^2/g.[3] The salt imbibition technique we report in this communication yields a stoichiometric 1:1 (Li:Al) precursor. Complete reaction to α-$LiAlO_2$ can be accomplished in the shortest time as well as at the lowest temperature because of the atomic scale mixing of components.

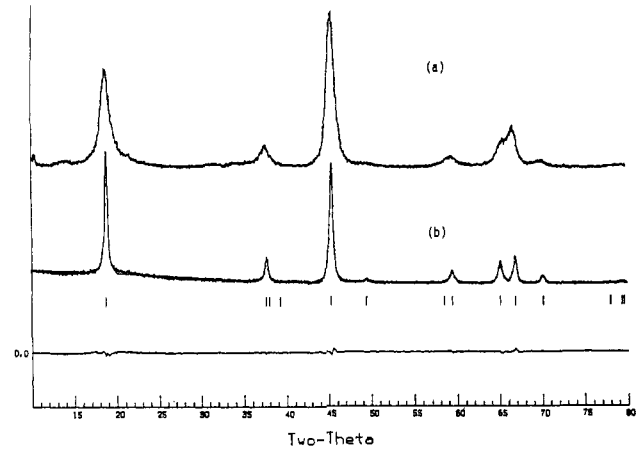

Figure 1. X-ray powder data for lithium monoaluminate calcined at 400 °C for 100 h (a) and refinement profile of polycrystalline α-$LiAlO_2$ (b). In the profile, dots are observed data and the solid line is the best-fit profile. The difference profile appears at the bottom.

Table I. Surface-Area and Pore-Size Data for α-$LiAlO_2$[a]

	SA, m^2/g	PS, Å	MPD, Å	APD, Å	TP, mL/g
400 °C/30 h	68	57	93	99	0.09
500 °C/1 h after 400 °C/30 h	68	59	94	103	0.07
400 °C/100 h	57	65	98	108	0.08
conventional method[b]	<5	138	NA	NA	NA

[a] Abbreviations: SA, specific surface area; PS, particle size; MPD, median pore diameter; APD, average pore diameter; TP, total porosity above 10 Å (radius). [b] Li_2CO_3 and AlO(OH) at 600 °C for 30 h.

The experimental procedure to imbibe $LiOH\cdot H_2O$ into $[LiAl_2(OH)_6]^+(OH)^-\cdot 2H_2O$ was performed by the same methodology as our original synthesis of the dialuminate.[1] Briefly, equimolar amounts of $[LiAl_2(OH)_6]^+(OH)^-\cdot 2H_2O$ and $LiOH\cdot H_2O$ were ground together and then left to react at room temperature under flowing nitrogen gas saturated with water vapor.[4] The product can also be prepared directly by reaction of $Al(OH)_3$ and $LiOH\cdot H_2O$. The reaction product, lithium monoaluminate ($LiAl(OH)_4\cdot nH_2O$; $0.9 \le n \le 1.3$), was identified by X-ray powder diffraction after several hours; however, several days were required for complete reaction. The formula $[LiAl_2(OH)_6]^+[Li(OH)_2\cdot H_2O]^-$ emphasizes that interlayer water of the dialuminate has been replaced by LiOH. No significant amount of an amorphous component was detected. The decomposition behavior of $LiAl(OH)_4\cdot nH_2O$ ($n \approx 1.0$) is very different compared to that of $LiAlO_2\cdot {}^1/_4H_2O$, which has been precipitated[5] from basic aqueous solution. $LiAlO_2\cdot {}^1/_4H_2O$ has an X-ray powder pattern very similar to that of β-$LiAlO_2$ and converts to β-$LiAlO_2$ upon calcination, whereas $LiAl(OH)_4\cdot nH_2O$ ($n \approx 1.0$) converts to α-$LiAlO_2$. Further experimental details will be published separately.

Figure 1 shows the X-ray powder diffraction pattern of α-$LiAlO_2$ prepared at 400 °C for 100 h (curve a), compared with the same material synthesized by the conventional route from Li_2CO_3 and AlO(OH) reacted at 600 °C for 30 h (curve b). In contrast, calcination for 1 h at 500 °C yielded mainly the β-phase. It is noteworthy that β-$LiAlO_2$ remains undetectable at 500 °C if the α-phase is first nucleated with prolonged heating at 400 °C.

The surface area of α-$LiAlO_2$ was studied by the BET method.[6] Median and average pore diameters were calculated by using the

(1) Poeppelmeier, K. R.; Hwu, S.-J. *Inorg. Chem.* **1987**, *26*, 3297.
(2) Kinoshita, K.; Sim, J. W.; Ackerman, J. P. *Mater. Res. Bull.* **1978**, *13*, 445.
(3) Poeppelmeier, K. R.; Kipp, D. O. *Inorg. Chem.* **1988**, *27*, 766.
(4) Hwu, S.-J.; Chiang, C. K. Unpublished work.
(5) Kolesova, V. A.; Sachenko-Sakun, L. K.; Guseva, I. V. *Russ. J. Inorg. Chem. (Engl. Transl.)* **1967**, *12*, 1704.
(6) Brunauer, S.; Emmett, P. H.; Teller, E. *J. Am. Chem. Soc.* **1938**, *60*, 309.

0020-1669/88/1327-4523$01.50/0